

Analytic Stability Theory for Faraday Waves and the Observation of the Harmonic Surface Response

H. W. Müller,¹ H. Wittmer,¹ C. Wagner,² J. Albers,² and K. Knorr²

¹*Institut für Theoretische Physik, Universität des Saarlandes, Postfach 151150, D 66041 Saarbrücken, Germany*

²*Institut für Technische Physik, Universität des Saarlandes, Postfach 151150, D 66041 Saarbrücken, Germany*

(Received 14 August 1996)

We present an analytic expression for the onset of the Faraday instability, which is applicable to a wide frequency range covering both shallow gravity and deep capillary waves. For sufficiently thin fluid layers, the surface oscillates in harmonic rather than subharmonic resonance with the forcing. An experimental confirmation of this result is reported. [S0031-9007(97)02704-X]

PACS numbers: 47.20.Ma, 47.15.Cb, 47.20.Gv

The observation of standing waves at the surface of a fluid layer subject to a vertical vibration dates back to Faraday [1]. For sufficiently strong driving, the plane surface undergoes an instability which gives rise to ordered wave patterns [2–4]. With a sinusoidal driving force, spatially periodic patterns [5–7], and quasiperiodic structures of eightfold or tenfold orientational order have been observed [8]. Faraday already recognized that the response of the surface is subharmonic; i.e., it appears with twice the period of the drive. The first investigation of the linear stability [9] showed that the problem can be reduced to a set of Mathieu oscillators. However, the analysis relies on the potential flow approximation which is restricted to inviscid fluids only. Viscous effects are usually treated by a heuristic damping in the Mathieu equation [10], proportional to the kinematic viscosity ν . This approximation ignores viscous boundary layers along the container walls and beneath the surface, where additional dissipation occurs. Beyer and Friedrich [11] showed that the surface boundary layer gives rise to a memory kernel in the Mathieu equation. Since they used the idealized free slip boundary conditions, they did not catch the dominating damping in the bottom boundary layer. The most advanced theoretical investigation of the stability problem [12] is fully numerical, which renders a physical understanding difficult. An analytic approach which accounts for the different competing damping mechanisms is still missing. Recently, Kumar [13] presented an approximation for weakly damped Faraday waves based on a truncation of the numerical method [12]. Besides being rather implicit (a numerical minimization of the neutral stability curve is still required), his approach is not systematic since it is unclear to what order of viscosity the obtained result is valid [14]. He points out the very interesting possibility of a synchronous (= harmonic) rather than subharmonic surface resonance, if the wavelength $\lambda = 2\pi/k$ becomes comparable to the filling depth h . In this situation, the dissipation in the bottom boundary layer becomes dominant. Kumar could not determine the parameter region for the harmonic response by analytic means; instead he presented a numerical example.

In the present Letter we develop a systematic perturbative treatment of the linear stability problem. We provide an analytic expression for the onset acceleration a_c and the critical wave number k_c . Also covered is the case of shallow water waves ($\lambda \approx h$), where earlier approximations [10] fail. Our formula allows a direct interpretation of the competing dissipation mechanisms. The subharmonic instability, which dominates over most of the driving frequency range, is perfectly reproduced by our expression. We also supply a formula for the harmonic threshold, which gives an estimate for the bicriticality. Finally, we report on the first experimental observation of Faraday waves in *harmonic* resonance with the forcing.

We consider a layer of an incompressible fluid of density ρ , depth h with a free upper surface in contact with air. The layer is subject to a sinusoidal vertical vibration corresponding to a modulated gravitational acceleration $g(t) = g_0 + a \cos 2\Omega t$ in a frame of reference comoving with the container. Control parameters are the modulation amplitude a and the drive frequency $f = 2\Omega/(2\pi)$. The free surface is initially flat at the vertical coordinate $z = 0$. As the drive amplitude exceeds a_c , the surface elevation $z = \zeta(x, y, t)$ oscillates, where x, y are the horizontal coordinates and t is the time. For fluids of viscosity ν and of depth h , the linear dispersion relation [13] for *free* (i.e., $a = 0$) surface waves of the form $\zeta \propto \exp i(kx - \omega t)$ is

$$0 = A(k, \omega) = \omega_0^2(k) + \frac{r(r^4 + 2r^2 + 5) \coth rkh - (1 + 6r^2 + r^4) \tanh kh}{r \coth rkh - \coth kh} \varepsilon^2 - \frac{4r(r^2 + 1) \tanh kh / (\sinh kh \sinh rkh)}{r \coth rkh - \coth kh} \varepsilon^2, \quad (1)$$

with $\omega_0^2(k) = \tanh kh [g_0 k + (\sigma/\rho)k^3]/\Omega^2$, $\varepsilon = \nu k^2/|\Omega|$, and $r = \sqrt{1 + i\omega/\varepsilon}$. The square root with the positive real part is accepted. For shorter notation, we have nondimensionalized time t and frequencies ω, ω_0 by referring to the control parameter Ω . In the ideal fluid limit $\nu \rightarrow 0$, Eq. (1) reduces to the well-known

gravity-capillary dispersion relation $\omega^2 = \omega_0^2(k)$. The parametric drive, introduced by replacing g_0 by $g(t)$, couples different temporal Fourier modes. The following linear evolution equation for the Fourier transform $\hat{\zeta}(\omega) = \int \exp(-i\omega t)\zeta(t) dt$ of the surface elevation is obtained:

$$A(k, \omega)\hat{\zeta}(\omega) + \frac{ak \tanh kh}{2\Omega^2} [\hat{\zeta}(\omega - 2) + \hat{\zeta}(\omega + 2)] = 0. \tag{2}$$

There are several relevant length scales in the problem (see Fig. 1): The wavelength $\lambda = 2\pi/k$ of the surface pattern, the thickness of the viscous boundary layer $\delta = \sqrt{2\nu/|\Omega|}$, and the capillary length $\sqrt{\sigma/(\rho g_0)}$, where σ is the surface tension. The geometry of the experiment enters via the filling depth h . We ignore the lateral dimension of the vessel L by assuming $L \rightarrow \infty$.

For analytic progress, we confine ourselves to the weak dissipation limit $\varepsilon \ll 1$, which means that the depth of the viscous boundary layer is small compared to the wavelength. Furthermore, we assume that h is at least a few times larger than the thickness of the viscous boundary layer, $h/\delta \gtrsim 3$, i.e., $\coth rkh \approx 1$ and $1/\sinh rkh \approx 0$. Note that there is no restriction upon the relation between h and λ . The two simplifications made are not very restrictive and our approach is applicable to almost all recent experiments. We first expand Eq. (1) in powers of $1/r = O(\sqrt{\varepsilon})$ giving

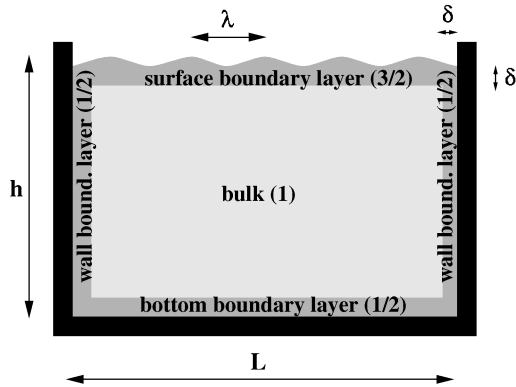


FIG. 1. Length scales of relevance: wavelength of the pattern $\lambda = 2\pi/k$, thickness of the viscous boundary layer $\delta = \sqrt{2\nu/|\Omega|}$, depth of the layer h , and lateral extension of the container L . Energy dissipation in the various regions scales with different powers of the viscosity ν (exponents are indicated in parentheses).

$$A(k, \omega) = \omega_0^2 - \omega^2 + i\omega\varepsilon(3 + \coth^2 kh) + \frac{\varepsilon^{1/2}(\varepsilon + i\omega)^{3/2}}{\sinh kh \cosh kh} + \varepsilon^{3/2}\sqrt{\varepsilon + i\omega} \times (-6 \tanh kh + \coth kh + \coth^3 kh) + \dots \tag{3}$$

The transformation of Eq. (3) into real space yields a damped Mathieu oscillator with nonlocal contributions [15]

$$0 = \ddot{\zeta}(t) + \varepsilon(3 + \coth^2 kh)\dot{\zeta}(t) + \left[\omega_0^2 + \frac{ak \tanh kh}{\Omega^2} \cos(2t) \right] \zeta(t) + \frac{\varepsilon^{1/2}}{\sqrt{\pi} \sinh kh \cosh kh} \int_{-\infty}^t G(t - \tau) (\varepsilon + \partial_\tau)^2 \zeta(\tau) d\tau + \frac{-6 \tanh kh + \coth kh + \coth^3 kh}{\sqrt{\pi}} \varepsilon^{3/2} \int_{-\infty}^t G(t - \tau) (\varepsilon + \partial_\tau) \zeta(\tau) d\tau, \tag{4}$$

where $G(t) = \exp(-\varepsilon t)/\sqrt{t}$ is the kernel. Besides the usual damping $\propto \dot{\zeta}$, which is related to the dissipation in the bulk, the two integrals also contribute to the damping: The moving surface emits velocity waves into the interior of the fluid, where history dependent dissipation occurs. The first memory integral scales like $O(\nu^{1/2})$ and is the leading dissipative contribution in the shallow water limit $kh = O(1)$. This expression is associated with the damping in the bottom boundary layer and dies out exponentially as kh increases. The second

integral (cf. Ref. [11]) remains for $h \rightarrow \infty$; it scales with $\nu^{3/2}$ and is related to the vortical flow field in the free surface boundary layer.

To proceed with the linear stability analysis, we expand the square roots in Eq. (3) giving

$$A(k, \omega) = -\omega^2 + X(k, \omega) + \omega_0^2, \tag{5}$$

where all viscous contributions up to $O(\varepsilon^{3/2})$ are collected in

$$X(k, \omega) = \Re(X) + i\Im(X) = -\varepsilon^{1/2} \frac{\sqrt{2}|\omega|^{3/2}}{\sinh 2kh} + \varepsilon^{3/2} \frac{|\omega|^{1/2}}{2\sqrt{2}} (-15 \tanh kh + 5 \coth kh + 2 \coth^3 kh) + i \operatorname{sgn}(\omega) \left[\varepsilon^{1/2} \frac{\sqrt{2}|\omega|^{3/2}}{\sinh 2kh} + \varepsilon |\omega| (3 + \coth^2 kh) + \varepsilon^{3/2} \frac{|\omega|^{1/2}}{2\sqrt{2}} (-15 \tanh kh + 5 \coth kh + 2 \coth^3 kh) \right]. \tag{6}$$

We first investigate the subharmonic resonance of the surface elevation by introducing

$$\hat{\zeta}(\omega) = \alpha_1 \delta(\omega - 1) + \alpha_2 \delta(\omega + 1) + \hat{\zeta}_1 + \dots \tag{7}$$

in Eq. (2). Assuming a small detuning $\omega_0^2 - 1 = O(X)$, the solvability condition for $\hat{\zeta}_1 = O(X)$ yields the neutral stability curve

$$[X(k, 1) + (\omega_0^2 - 1)][X(k, -1) + (\omega_0^2 - 1)] = \left(\frac{ak \tanh kh}{2\Omega^2} \right)^2. \quad (8)$$

The minimum of the drive amplitude a with respect to ω_0^2 [16] defines the onset of the subharmonic response

$$a_c^{(S)} \approx \frac{2\Omega^2}{k_S} \Im[X(k_S, 1)] \coth k_S h. \quad (9)$$

The critical wave number k_S results from the dispersion relation with a viscous detuning

$$\omega_0^2(k_S) \approx 1 - \Re[X(k_S, 1)]. \quad (10)$$

For water and for a viscous silicone oil Fig. 2 compares the analytic formula Eq. (9) with the full numerical computation [12]. Excellent agreement is achieved over a wide frequency range. Equation (9) serves as a simple and reliable substitute for the numerical solution of the stability problem. The three contributions in $\Im(X)$ [Eq. (6)] are related, respectively, to damping in the bottom boundary layer, the bulk, and the surface boundary layer, which dominate at low, intermediate, and higher drive frequencies. Even the sharp increase of the subharmonic onset towards lower frequencies (shallow water limit $kh \approx 1$) is well reproduced.

A similar perturbation expansion can be computed for the first *harmonic* stability tongue. We obtain for the

onset amplitude

$$a_c^{(H)} \approx \frac{4\Omega^2}{k_H} \sqrt{\Im[X(k_H, 2)]} \coth k_H h \quad (11)$$

with the critical wave number k_H determined by

$$\omega_0^2(k_H) \approx 4 + \frac{2}{3} \Im[X(k_H, 2)] - \Re[X(k_H, 2)]. \quad (12)$$

The two thresholds $a_c^{(S)}$ and $a_c^{(H)}$ intersect at a bicriticality (see Fig. 2), below which the harmonic response preempts the subharmonic one. The agreement between $a_c^{(H)}$ and the numerical result is not as good as in the subharmonic case. This is because the expansion for $a_c^{(H)}$ proceeds in powers of $X^{1/2}$, while it goes as X^1 for $a_c^{(S)}$. In the neighborhood of the bicriticality the nondimensional damping coefficient $\Im(X(k_H, 2))$ exceeds unity rendering the perturbation expansion invalid in this region.

The harmonic surface response is difficult to observe experimentally. The appropriate Ω window is rather narrow and occurs at very low excitation frequencies f . For f below ≈ 10 Hz it is usually the maximum peak *elevation* (rather than the maximum *force*) which prevents the shaker from reaching the threshold amplitude $a_c^{(H)}$. As shown in the inset of Fig. 2, the bicritical point tends towards higher frequencies as the viscosity of the fluid is increased. We therefore have set up an experiment with a viscous silicone oil (Dow Corning 200). At the working temperature of $T = 30^\circ\text{C}$ the viscosity amounts $\nu = 8.9 \text{ mm}^2/\text{s}$, surface tension $\sigma = 19.8 \times 10^{-3} \text{ N/m}$, and density $\rho = 0.929 \text{ g/cm}^3$. We use a cylindrical aluminum container of radius $R = 45 \text{ mm}$ and depth $h = 5 \text{ mm}$. Between a radius of 35 mm and the outer edge, the depth profile decreases continuously to zero to damp meniscus waves. An electromagnetic shaker V400 (LDS) is used with a maximum force of 98 N and a peak elevation of 8 mm, as specified by the manufacturer. Wave form generation as well as data acquisition is performed by a personal computer. The acceleration is measured by a piezoelectric device (Bruel and Kjaer 4393). For pattern visualization the container is illuminated stroboscopically from above by a concentric ring (20 cm in diameter) of 50 high intensity light emitting diodes (LED). A CCD camera located in the middle of the ring observes the pattern from the top. The LEDs are synchronized to the drive and triggered with either Ω or 2Ω . This technique allows a clear distinction between the subharmonic and harmonic surface resonance. As explained above, bottom damping is crucial for the harmonic Faraday instability. This requires a depth to wavelength ratio of $kh \lesssim 1$. In our experiment we use a filling depth of $h \approx 0.8 \text{ mm}$. For this combination of parameters the stability theory predicts the harmonic-subharmonic bicriticality, $a_c^{(S)} = a_c^{(H)}$, at $f \approx 9 \text{ Hz}$, which is close to the low frequency limit of our apparatus. Figure 3(a) presents a photograph of a pattern in harmonic resonance with

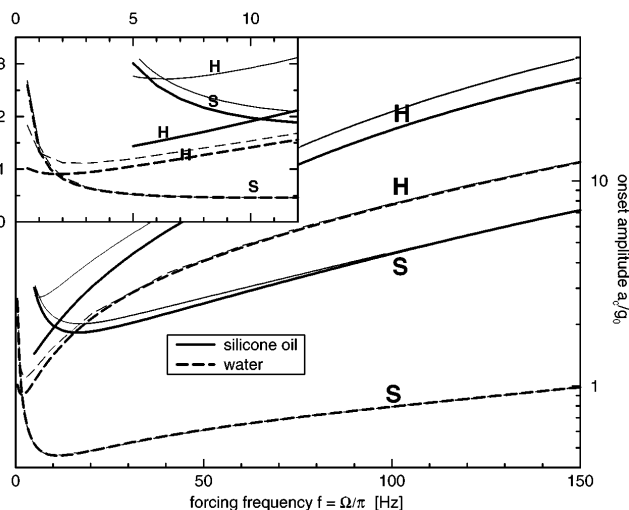


FIG. 2. The critical onset amplitude for the subharmonic (S) and harmonic (H) Faraday instability as a function of the forcing frequency $f = \Omega/\pi$. Thick lines correspond to the analytic results [Eqs. (9) and (11)]; thin lines are obtained by an exact numerical treatment. Parameters for water (dashed): $\rho = 1.0 \text{ g/cm}^3$, $\sigma = 72.4 \times 10^{-3} \text{ N/m}$, $\nu = 1 \text{ mm}^2/\text{s}$, $h = 1 \text{ mm}$; for silicone oil (solid): $\rho = 0.934 \text{ g/cm}^3$, $\sigma = 20.1 \times 10^{-3} \text{ N/m}$, $\nu = 10 \text{ mm}^2/\text{s}$, $h = 1 \text{ mm}$.

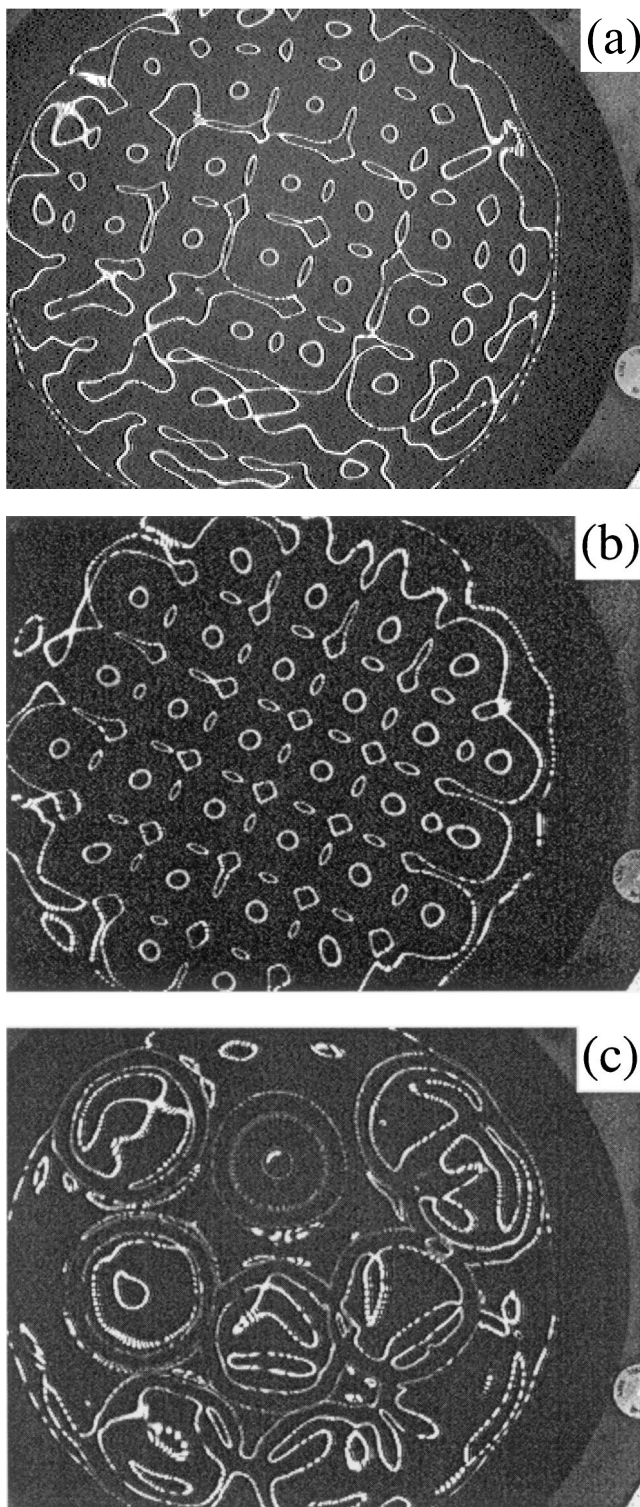


FIG. 3. Surface patterns as observed in the experiment. (a) Driving force and surface oscillate synchronously at $f = 9$ Hz (harmonic response). (b) Subharmonic surface response with 9 Hz at a drive with $f = 18$ Hz. (c) Subharmonic surface oscillation with 5 Hz at a drive with $f = 10$ Hz.

the drive. Both, the vessel and the surface are oscillating synchronously with 9 Hz. To confirm our observation

we show in Fig. 3(b) a subharmonic surface pattern, oscillating again with 9 Hz but excited with $f = 18$ Hz. As expected, the wavelength in Figs. 3(a) and 3(b) are the same. Finally, Fig. 3(c) depicts a subharmonic pattern driven at $f = 10$ Hz exhibiting a considerably larger wavelength. All patterns have been obtained by slowly increasing the drive amplitude a beyond the threshold while keeping f constant. The small aspect ratio of our container (diameter to wavelength ratio) did not allow the observation of well ordered structures [17].

In summary, we have presented analytic expressions for the onset of subharmonic Faraday waves in perfect agreement with the numerical solution. The analysis is based on the low viscosity approximation and assumes a filling depth larger than the thickness of the viscous boundary layer. Almost all recent experiments reported in the literature are covered by these assumptions. Particularly interesting is the case of shallow water waves ($\lambda \approx h$) for which the harmonic instability preempts the subharmonic one. This theoretical prediction is confirmed by an experiment.

Fruitful discussions with S. Fauve are gratefully acknowledged. This work is supported by the Deutsche Forschungsgemeinschaft.

-
- [1] M. Faraday, *Philos. Trans. R. Soc. London* **52**, 319 (1831).
 - [2] N.B. Tuffillaro, R. Ramshankar, and J.P. Gollub, *Phys. Rev. Lett.* **62**, 422 (1989).
 - [3] J.W. Miles and D. Henderson, *Annu. Rev. Fluid Mech.* **22**, 143 (1990).
 - [4] J.P. Gollub, *Physica (Amsterdam)* **51**, 501 (1991).
 - [5] S. Douady, *J. Fluid Mech.* **221**, 383 (1990).
 - [6] W.S. Edwards and S. Fauve, *J. Fluid Mech.* **278**, 123 (1994).
 - [7] K. Kumar and K.M. Bajaj, *Phys. Rev. E* **52**, R4606 (1995).
 - [8] B. Christiansen, P. Alstrom, and M.T. Levinsen, *Phys. Rev. Lett.* **68**, 2157 (1992); D. Biulis and W. van de Water, *Phys. Rev. Lett.* (to be published).
 - [9] T.B. Benjamin and F. Ursell, *Proc. R. Soc. London A* **225**, 505 (1954).
 - [10] L. Landau and E.M. Lifshitz, *Fluid Mechanics* (Pergamon Press, New York, 1987), 2nd ed.
 - [11] J. Beyer and R. Friedrich, *Phys. Rev. E* **51**, 1162 (1995).
 - [12] K. Kumar and L.S. Tuckerman, *J. Fluid Mech.* **279**, 49 (1994).
 - [13] K. Kumar, *Proc. R. Soc. London A* **452**, 1113 (1996).
 - [14] A.H. Nayfeh and D.T. Mook, *Nonlinear Oscillations* (Wiley, New York, 1979).
 - [15] To transform $\sqrt{\varepsilon + i\omega}$ and $\sqrt{\varepsilon + i\omega}^3$ into real space use the identity $1/\sqrt{\pi} \int_0^\infty u^{-1/2} \exp[-(\varepsilon + i\omega)u] du = (\varepsilon + i\omega)^{-1/2}$.
 - [16] Up to $O(X)$ minimization with respect to either k or ω_0^2 is equivalent.
 - [17] For the harmonic surface resonance [Fig. 3(a)], we had to drive the shaker to elevations 50% above the maximum specified by the manufacturer. Note, however, that the $2f$ distortion of the container vibration did not exceed 2%.